C-M-C (axial) 180°; in Ru compounds with phosphido bridges Ru-P = 2.3 Å; in $Ni_4(\mu\text{-SH})_8$ Ni-S = 2.2 Å, S-H = 1.4 Å, Ni···Ni = 2.69 Å; in $[Pd_4(\mu\text{-CO})_4H_8]^{4-}$ Pd-Pd = 2.66 Å, Pd···Pd = 2.91 Å, Pd-C = 2.00 Å.

The three-dimensional graphics of the orbitals has been performed by a computer program named CACAO (Computer Aided Composition of Atomic Orbitals) written in fortran language by C. Mealli and D. M. Proserpio. A detailed description is reported elsewhere.[62]

(62) Mealli, C.; Proserpio, D. M. *J. Chem. Educ.* **1990**, *66*, 000.

Ferromagnetic Behavior of Linear Chain Electron-Transfer Complexes. Decamethylferrocene Electron-Transfer Salts of 2,5-Disubstituted-7,7,8,8-tetracyano-p-quinodimethanes. Magnetic Characterization of $[Fe(C_5Me_5)_2]^+[TCNQI_2]^-$ and Structures of $[TCNQI_2]^{n-}$ (n = 0, 1, 2)

Joel S. Miller,[*,1a] **Joseph C. Calabrese,**[1a] **Richard L. Harlow,**[1a] **David A. Dixon,**[*,1a] **Jian H. Zhang,**[1b] **William M. Reiff,**[*,1b] **Sailesh Chittipeddi,**[1c] **Mark A. Selover,**[1c] **and Arthur J. Epstein***[1c]

Contribution No. 5213 from the Central Research and Development Department, E. I. du Pont de Nemours & Co., Inc., Experimental Station E328, Wilmington, Delaware 19880-0328, the Department of Physics and Department of Chemistry, The Ohio State University, Columbus, Ohio 43210-1106, and the Department of Chemistry, Northeastern University, Boston, Massachusetts 02115. Received November 9, 1989

Abstract: The reaction of $Fe(C_5Me_5)_2$ donor (D) and 2,5-disubstituted-7,7,8,8-tetracyano-p-quinodimethane, $TCNQR_2$ (R = Cl, Br, I, Me, OMe, OPh) acceptor (A), results in the formation of 1:1 electron-transfer complexes of $[Fe(C_5Me_5)_2]^{\cdot+}[TCNQR_2]^{\cdot-}$ composition. The structure of $[Fe(C_5Me_5)_2]^{\cdot+}[TCNQI_2]^{\cdot-}$ belongs to the centrosymmetric $P2_1/n$ space group [a = 11.131 (2) Å, b = 32.929 (5) Å, c = 8.728 (1) Å, β = 105.06 (1)°, Z = 4, V = 3089 Å³, R = 3.4%; R_w = 3.1% at -100 °C]. The unit cell comprises ···D⁺A⁻D⁺A⁻D⁺A⁻··· chains along a with the intrachain $Fe^{III}···Fe^{III}$ distance of 11.131 Å and the interchain $Fe^{III}···Fe^{III}$ separations less than the intrachain spacing of 8.728 (in-registry) and 9.778 Å (out-of-registry). The cation's C_5 rings are nearly eclipsed (4°); thus it possesses approximate D_{5h} symmetry with the average bond distances comparable to those previously reported for $[Fe(C_5Me_5)_2]^{\cdot+}$. The structure of {[Co(C₅Me₅)₂]⁺}₂[TCNQI₂]²⁻ belongs to the centrosymmetric $P\bar{1}$ space group [a = 9.537 (3) Å, b = 9.880 (2) Å, c = 12.728 (1) Å, α = 85.24 (1)°, β = 86.25 (1)°, γ = 81.39 (2)°, Z = 1, V = 1180 Å³, R = 5.4%; R_w = 5.5% at -70 °C]. The unit cell comprises ···D⁺A²⁻D⁺D⁺A²⁻D⁺··· chains of diamagnetic cations and anions. The cation's C_5 rings are staggered and possess approximate D_{5d} symmetry with the average bond distances comparable to those previously reported for $[Co(C_5Me_5)_2]^+$. The structures of $TCNQI_2$, S = ½[TCNQI₂]˙⁻, and [TCNQI₂]²⁻ possessing local C_{2h}, C_i, and C_i symmetries, respectively, have been determined for the first time. The average distances are r(HC=Cl) = 1.356, 1.348, 1.384; r(IC-C) = 1.449, 1.438, 1.411; r(HC-C) = 1.445, 1.428, 1.384; r[C=C(CN)₂] = 1.388, 1.409, 1.458; r(C-CN) = 1.435, 1.423, 1.410; and r(C≡N) = 1.144, 1.144, 1.137 Å for $TCNQI_2$, [TCNQI₂]˙⁻, and [TCNQI₂]²⁻, respectively. Although $TCNQI_2$ is nearly planar, the -C(CN)₂ groups of [TCNQI₂]˙⁻ are rotated by 9 and 16° from the C_6 plane and the -C(CN)₂ groups of [TCNQI₂]²⁻ are rotated by 26° from the C_6 plane. Above 60 K the magnetic susceptibility of the [TCNQI₂]˙⁻ salt obeys the Curie-Weiss expression (θ = +9.5 K; μ_{eff} = 3.96 μ_B), and this electron-transfer salt has dominant ferromagnetic interactions. Above 10 K this complex exhibits classical low spin Fe(III) ferrocenium singlet ⁵⁷Fe Mössbauer spectra [isomer shift, δ = 0.474 mm/s (300 K) relative to iron foil; line width, Γ ~ 0.367 mm/s]. At 1.5 K a hyperfine pattern with six transitions is evident but poorly resolved. The spectrum corresponds to Zeeman splitting by an internal field of 270 kG reflecting an intermediate paramagnetic relaxation rate. The $[Fe(C_5Me_5)_2]^{\cdot+}[TCNQR_2]^{\cdot-}$ (R = Cl, Br, Me, OMe, OPh) salts exhibit lower moments. Results from ab initio molecular orbital calculations on [TCNQI₂]ⁿ⁻ (n = 0, 1, 2) are presented as an aid to interpreting experiment.

Introduction

Linear chain, 1-D, complexes containing strong acceptors have been shown over the past quarter of a century to frequently exhibit unusual electronic, particularly electrical, properties.[2-4] In 1979

we reported[5] metamagnetic behavior for the 1-D phase of $[Fe(C_5Me_5)_2]^{\cdot+}[TCNQ]^{\cdot-}$ [TCNQ = 7,7,8,8-tetracyano-p-quino-dimethane]. Metamagnetism involves the field dependent switching from the antiferromagnetic state to a low-lying ferromagnetic state. It is an unusual property for a molecular solid which does not possess any interion interactions less than the sum

(1) (a) Du Pont Co. (b) Northeastern University. (c) Ohio State University.

(2) For a detailed overview, see the proceedings of the recent series of international conferences: *Syn. Met.* **1988**, *27*; **1989**, *28*, *29* (Aldissi, M., Ed.). *Mol. Cryst. Liq. Cryst.* **1985**, *117-121* (Pecile, C., Zerbi, G., Bozio, R., Girlando, A., Eds.). *J. Phys. (Paris) Collogue* **1983**, *44-C3* (Comes, R., Bernier, P., Andre', J. J., Rouxel, J., Eds.). *Mol. Cryst. Liq. Cryst.* **1981**, *77*, *79*, *82*, *83*, *85*; **1982**, *86* (Epstein, A. J., Cornwell, E. M., Eds.). *Chem. Scr.* **1981**, *17* (Carneiro, K., Ed.). *Lecture Notes Physics* **1979**, *95* and *96* (Bartsic, S., Bjelis, A., Cooper, J. R., Leontic, B. A., Eds.). *Ann. N.Y. Acad. Sci.* **1978**, *313* (Miller, J. S., Epstein, A. J., Eds.).

(3) Epstein, A. J.; Miller, J. S. *Sci. Am.* **1979**, *240*(no. 4), 52. Bechgaard, K.; Jerome, D. *Sci. Am.* **1983**, *247*(no. 2), 52.

(4) See, for example: *Extended Linear Chain Compounds*; Miller, J. S., Ed.; Plenum Publisher Corporation: New York, 1982 and 1983; Vols. 1-3. Simon, J.; Andre, J. J. *Molecular Semiconductors*; Springer Verlag: NY, 1985.

(5) Candela, G. A.; Swartzendruber, L.; Miller, J. S.; Rice, M. J. *J. Am. Chem. Soc.* **1979**, *101*, 2755.

Table I. Summary of Elemental Analysis, $\nu(C\equiv N)$ Infrared Spectral Data, and Unit Cell Parameters for [Fe(C$_5$Me$_5$)$_2$]$^{\cdot+}$[TCNQR$_2$]$^{\cdot-}$

anion	TCNQCl$_2$	TCNQBr$_2$	TCNQI$_2$	TCNQMe$_2$	TCNQ(OMe)$_2$	TCNQ(OPh)$_2$	TCNQMeCl
% C, calc	64.13	55.84	49.13	73.11	69.15	73.94	68.46
% C, obs	64.19	56.02	49.47	73.01	68.89	73.50	68.20
% H, calc	5.38	4.69	4.12	6.86	6.49	5.92	6.09
% H, obs	5.40	4.69	4.34	6.60	6.45	5.83	5.54
% N, calc	9.35	8.14	7.16	10.03	9.49	7.84	9.68
% N, obs	9.14	7.99	7.24	10.17	9.97	7.78	9.71
mw	599.36	688.30	782.29	558.56	590.56	968.51	578.97
a, Å		7.48	11.13	3.87			
b, Å		14.87	32.929	9.15			
c, Å		26.68	8.728	28.5			
α, deg		88.18	90.0	90.0			
β, deg		82.18	105.06	90.0			
γ, deg		81.04	90.0	90.0			
volume, V, Å^3		2906.0	3143.0	1011.50			
unit cell		triclinic	monoclinic	orthorhombic			
μ_{eff} (293 K), μ_B	3.02	3.00	3.96	2.28	2.74	3.64	3.49
θ, K	+4.3	+0.12	+9.5	−6.2	2.09	−1.5	0.15

of the van der Waals separations.[6] As part of our ongoing investigations of cooperative behavior in organic based molecular solids, we have deliberately sought to prepare electron-transfer complexes possessing a ferromagnetic ground state in order to understand the fundamental phenomena governing meta- and ferromagnetism.[7] Hence, we have undertaken the systematic study of the structure-function relationship between salts comprised primarily of metallocenium cations and planar polycyano acceptors with the goal of elucidating the electronic and steric requirements for the stabilization of the meta- and ferromagnetic states.

Replacement of the radical anion in a [Fe(C$_5$Me$_5$)$_2$]$^{\cdot+}$ salt provides a means to study structure-function relationships.[7e,8] This should provide insight into the crucial steric/electronic features which stabilize ferromagnetic coupling as well as stabilize bulk ferromagnetic behavior. Utilizing TCNE (TCNE = tetra-cyanoethylene) as its Fe(C$_5$Me$_5$)$_2$ electron-transfer salt, we have demonstrated the occurrence of a bulk ferromagnet.[7,9] Previously we have reported that [Fe(C$_5$Me$_5$)$_2$]$^{\cdot+}$ salts of 2,3-dichloro-4,5-dicyanobenzoquinoneide,[10] [DDQ]$^{\cdot-}$, {Ni[S$_2$C$_2$(CF$_3$)$_2$]$_2$}$^{\cdot-}$,[11] and [C$_4$(CN)$_6$]$^{\cdot-}$[12] exhibit ferromagnetic coupling; however, they do not exhibit bulk ferromagnetic behavior. Thus, although the gross structural $\cdots$D$^{\cdot+}$A$^{\cdot-}$D$^{\cdot+}$A$^{\cdot-}$D$^{\cdot+}$A$^{\cdot-}\cdots$ motif is maintained, subtle changes in the interior interactions substantially alter the magnetic properties. In order to better understand the relative importance of and competition between the inter- and intrachain interactions, we are systematically studying the effect of replacement of TCNQ with other radical anion acceptors and herein report our results on 2,5-disubstituted-TCNQ electron-transfer salts of Fe(C$_5$Me$_5$)$_2$.

---

(6) A molecular solid is a solid comprised of low molecular weight molecules or ions that do not possess extended covalent bonding in the solid state. However, interactions shorter than the sum of the van der Waal separations may be present in the solid. Dissolution into conventional aqueous or organic solvents should lead to solvation of the noninteracting ions or molecules that were used to prepare the molecular solid.

(7) (a) Miller, J. S.; Epstein, A. J.; Reiff, W. M. *Isr. J. Chem.* **1987**, *27*, 363. (b) Miller, J. S.; Epstein, A. J.; Reiff, W. M. *Chem. Rev.* **1988**, *88*, 201. (c) Miller, J. S.; Epstein, A. J.; Reiff, W. M. *Acc. Chem. Res.* **1988**, *21*, 114. (d) Miller, J. S.; Epstein, A. J. *NATO ASI Ser. B* **1987**, *168*, 159. (e) Miller, J. S.; Epstein, A. J. *Mol. Cryst. Liq. Cryst.* **1989**, *176*, 347. (f) Miller, J. S.; Epstein, A. J. *New Aspects of Organic Chemistry*; Yoshida, Z., Shiba, T., Ohsiro, Y., Eds.; VCH Publishers: New York, NY, 1989; p 237.

(8) Broderick, W. E.; Thompson, J. A.; Godfrey, M. R.; Sabat, M.; Hoffman, B. M.; Day, E. P. *J. Am. Chem. Soc.* **1989**, *111*, 7656.

(9) (a) Miller, J. S.; Calabrese, J. C.; Dixon, D. A.; Epstein, A. J.; Bigelow, R. W.; Zhang, J. H.; Reiff, W. M. *J. Am. Chem. Soc.* **1987**, *109*, 769. (b) Miller, J. S.; Calabrese, J. C.; Epstein, A. J.; Bigelow, R. W.; Zhang, J. H.; Reiff, W. M. *J. Chem. Soc., Chem. Commun.* **1986**, 1026. (c) Chittipeddi, S.; Cromack, K. R.; Miller, J. S.; Epstein, A. J. *Phys. Rev. Lett.* **1987**, *22*, 2695.

(10) (a) Gebert, E.; Reis, A. H., Jr.; Miller, J. S.; Rommelmann, H.; Epstein, A. J. *J. Am. Chem. Soc.* **1982**, *104*, 4403. (b) Miller, J. S.; Krusic, P. J.; Dixon, D. A.; Reiff, W. M.; Zhang, J. H.; Anderson, E. C.; Epstein, A. J. *J. Am. Chem. Soc.* **1986**, *108*, 4459.

(11) Miller, J. S.; Calabrese, J. C.; Epstein, A. J. *Inorg. Chem.* **1989**, *28*, 4230.

(12) Miller, J. S.; Zhang, J. H.; Reiff, W. M. *J. Am. Chem. Soc.* **1987**, *109*, 4584.

Table II. X-ray Crystallography Parameters for TCNQI$_2$ [Fe(C$_5$Me$_5$)$_2$]$^{\cdot+}$[TCNQI$_2$]$^{\cdot-}$, and {[Co(C$_5$Me$_5$)$_2$]$^+$}$_2$[TCNQI$_2$]$^{2-}$

parameter	TCNQI$_2$	[TCNQI$_2$]$^{\cdot-}$	[TCNQI$_2$]$^{2-}$
formula	C$_{12}$H$_2$I$_2$N$_4$	C$_{32}$H$_{32}$FeI$_2$N$_4$	C$_{52}$H$_{62}$Co$_2$I$_2$N$_4$
formula wt	455.98	782.29	1114.76
space group	$P2_1/c$ (no. 14)	$P2_1/n$ (no. 14)	$P\bar{1}$ (no. 2)
a, Å	6.290 (1)	11.131 (2)	9.537 (3)
b, Å	6.477 (2)	32.929 (5)	9.880 (2)
c, Å	14.862 (3)	8.728 (2)	12.728 (1)
α, deg			85.24 (1)
β, deg	90.72 (1)	105.06 (1)	86.25 (1)
γ, deg			81.39 (2)
V, Å^3	605.4	3089.2	1180.0
Z	2	4	1
ρ, (calc) g cm^{-3}	2.501	1.682	1.566
crystal dimension, mm	0.13 × 0.12 × 0.43	0.15 × 0.05 × 0.45	0.25 × 0.16 × 0.41
temp, °C	−70	−100	−70
diffractometer	CAD4	Syntex R3	CAD4
radiation, λ, Å	Mo Kα 0.71073	Mo Kα 0.71073	Mo Kα 0.71073
absorption coeff, cm^{-1}	51.24	24.92	20.31
2θ range, deg	$2.7 < 2\theta < 60$	$4.5 < 2\theta < 48$	$3.2 < 2\theta < 52$
scan type	θ–2θ	ω	ω
total data	1893	5218	4820
absorption correction	ψ-scan	ψ-scan	ψ-scan
data I > 3σ(I)	1546	3197	3445
parameters	86	352	271
R (F_o^2)	0.019	0.035	0.54
R_w (F_o^2)	0.025	0.033	0.55
residual electron den., Å^{-3}	0.69 I(1)	0.56 H(29)	1.66 I(1)

Experimental Section

[Fe(C$_5$Me$_5$)$_2$]$^{\cdot+}$[TCNQI$_2$]$^{\cdot-}$ was prepared from Fe(C$_5$Me$_5$)$_2$ (Strem Chemical Co.) and 2,5-diiodo-7,7,8,8-tetracyano-p-quinodimethane, TCNQI$_2$.[13] [Fe(C$_5$Me$_5$)$_2$][TCNQI$_2$] was prepared in an inert atmosphere glovebox by reaction of decamethylferrocene (86 mg, 0.26 mmol) dissolved in 10 mL of hot acetonitrile with 120 mg (0.26 mmol) of TCNQI$_2$ also in 60 mL of hot MeCN. After refrigeration at −25 °C overnight, 110 mg of product (55%) was collected via vacuum filtration. Elemental analysis are in Table I.

[Fe(C$_5$Me$_5$)$_2$]$^{\cdot+}$[TCNQR$_2$]$^{\cdot-}$. Other 2,5-disubstituted-7,7,8,8-tetra-cyano-p-quinodimethanes (TCNQR$_2$; R = Br, Cl, Me, OMe, OPh, as well as TCNQMeCl) were prepared by the above method with different TCNQR$_2$.[13] Elemental analysis and unit cell parameters are listed in Table I. Crystals suitable for single-crystal X-ray diffraction could not be grown for these latter materials.

{[Co(C$_5$Me$_5$)$_2$]$^+$}$_2$[TCNQR$_2$]$^{2-}$ was prepared from 50 mg (0.153 mmol) of Co(C$_5$Me$_5$)$_2$ dissolved in 25 mL of hot acetonitrile and 35 mg (0.076 mmol) of TCNQI$_2$ dissolved in 75 mL of hot acetonitrile. After addition

---

(13) Wheland, R. C.; Martin, E. L. *J. Org. Chem.* **1975**, *40*, 3101.

of the donor to the acceptor the mixture turned black-green and upon reducing the volume to 10 mL and cooling to room temperature green-black crystals were deposited and collected by vacuum filtration and dried (40 mg, 47%). Anal. Calcd for $C_{52}H_{62}CoI_2N_4$ (Found) C = 56.03 (55.92), H = 5.61 (5.28), and N = 5.03 (5.46).

X-ray Data Collection, Reduction, Solution, and Refinement. The single-crystal X-ray structures of TCNQI$_2$, [Fe(C$_5$Me$_5$)$_2$]$^{\bullet+}$[TCNQI$_2$]$^{\bullet-}$, and {[Co(C$_5$Me$_5$)$_2$]$^+$}$_2$[TCNQR$_2$]$^{2-}$ were solved by standard techniques. Key parameters for the data collection, data reduction, solution, and refinement are summarized in Table II. The fractional coordinates, anisotropic thermal parameters, general temperature factors, and cation bond distances and angles are included as supplementary material. ORTEP and CHEM-X were used to generate some of the figures presented in this paper.[34]

The structure for TCNQI$_2$ was solved by the Patterson heavy-atom method which yielded the position of an I atom. The remaining atoms were located in subsequent Fourier difference maps. The molecule is located on the special position ⟨0, 0, 1/2⟩ with site symmetry 1̄. The unique hydrogen atom position was refined. The structure for the [TCNQI$_2$]$^{\bullet-}$ salt was solved via automated Patterson analysis. The non-hydrogen atoms were refined anisotropically, and all hydrogen atoms were fixed. The rotational orientation of the methyl hydrogens were idealized from early least-squares refined positions. The structure of the dianion complex was also solved by the Patterson method. Early attempts to refine the hydrogen atoms were only partially successful, and once again the hydrogen atom positions were idealized. All other atoms were refined anisotropically. The dianion is located on a crystallographic inversion center. Neutral atom scattering factors and anomalous dispersion factors for Fe and I were taken from Cromer and Waber.[14]

[57]Fe Mössbauer Spectroscopy. Zero field Mössbauer spectra were determined by using a conventional constant acceleration spectrometer with a 50 mCi [57]Co source electroplated onto the surface and annealed into the body of the 6 μm thick foil of high purity rhodium in a hydrogen atmosphere. The details of cryogenics, temperature control, etc. have been described previously.[15]

Magnetic Measurements. The magnetization,[10a] M, and magnetic susceptibility, χ, were measured for powdered samples by using the Faraday technique which has been previously described.[10] The contributions of the sample holder, ferromagnetic impurities (obtained with a Honda Analysis), and the core diamagnetism[16] were subtracted in order to obtain the corrected data.

Molecular Orbital Calculations. The geometries of the closed shell species TCNQI$_2$ and [TCNQI$_2$]$^{2-}$ were gradient optimized[17] at the SCF level initially in C_{2h} symmetry. The STO-3G basis set[18] (140 basis functions) was used in the calculations with the exponents and coefficients for the I from the work of Hehre and co-workers.[18] Force fields were calculated analytically.[19] The above calculations were all done with the program GRADSCF[20] on a CRAY X-MP/24 computer system. Calculations on the [TCNQI$_2$]$^{\bullet-}$ were done with the program HONDO[21] on the CRAY X-MP computer in order to obtain charge distributions. These calculations were done with the geometries of TCNQI$_2$ and [TCNQI$_2$]$^{2-}$ and at an average of the two geometries (see supplementary material for coordinates). The averaged geometry was generated from the dianion geometry by appropriate lengthening and shortening of the bond distances. The charge and spin distributions for the radical anion were only
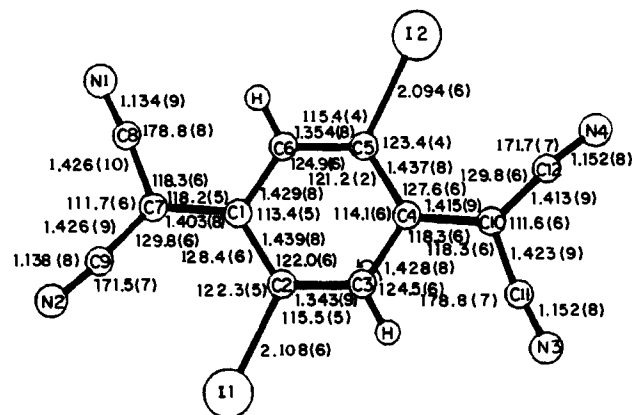
(14) (a) Cromer, D. T.; Waber, J. T. *International Tables for X-ray Crystallography*; The Kynoch Press: Birmingham, England, 1974; Vol. IV, Table 2.2B. (b) Cromer, D. T.; Waber, J. T. *International Tables for X-ray Crystallography*; The Kynoch Press: Birmingham, England, 1974; Vol. IV, Table 2.3.1.

(15) Cheng, C.; Reiff, W. M. *Inorg. Chem.* **1977**, *16*, 2097.

(16) The following diamagnetic corrections were used: Fe(C$_5$Me$_5$)$_2$ is –230 × 10^{-6} emu/mol;[10a] TCNQR$_2$ (R = Cl, Me) was determined to be –124 and –118 × 10^{-6} emu/mol, respectively. For TCNQR$_2$ (R = Br, I, OMe, OPh) the following values were calculated with Pascal constants: –153, –181, –127, and –209 × 10^{-6} emu/mol, respectively.
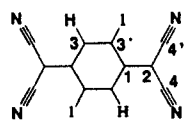
(17) (a) Pulay, P. In *Applications of Electronic Structure Theory*; Schaefer, H. F., III, Ed.; Plenum: New York, 1977; Chapter 4. (b) Komornicki, A.; Ishida, K.; Morokuma, K.; Ditchfield, R.; Conrad, M. *Chem. Phys. Lett.* **1977**, *45*, 595.

(18) Hehre, W. J.; Stewart, R. F.; Pople, J. A. *J. Chem. Phys.* **1969**, *51*, 2657.

(19) (a) King, H. F.; Komornicki, A. *J. Chem. Phys.* **1986**, *84*, 5645. (b) King, H. F.; Komornicki, A. In *Geometrical Derivatives of Energy Surfaces and Molecular Properties*; Jørgenson, P., Simons, J., Eds.; NATO ASI Series C, D. Reidel: Dordrecht, 1986; Vol. 166, p 207.

(20) GRADSCF is an ab initio gradient program system designed and written by A. Komornicki at Polyatomics Research Mountain View, CA.

(21) Dupuis, M.; Rys, J.; King, H. F. *J. Chem. Phys.* **1976**, *65*, 111. King, H. F.; Dupuis, M.; Rys, J. *National Resource for Computer Chemistry Software Catalog*; Progrm QH02 (HONDO), 1980; Vol. 1.

Figure 1.   Atom labeling, bond distances, and bond angles for [TCNQI$_2$]$^{\bullet-}$ in [Fe(C$_5$Me$_5$)$_2$]$^{\bullet+}$[TCNQI$_2$]$^{\bullet-}$.

weakly dependent of the starting geometry.

Results and Discussion

Crystal Structure—TCNQI$_2$. The atom designations, bond distances, and bond angles for TCNQI$_2$ are located in Table III. TCNQI$_2$ is approximately planar (C_{2h} symmetry) with a small twist of 4° of the planes containing the C(CN)$_2$ groups about the exocyclic double bonds. The C$_3$C$_3'$ bond is 0.018 Å longer than the bond in TCNQ,[22] and the C$_3$–C$_1$ bonds are 0.006 Å longer in TCNQI$_2$. Thus the ring is slightly expanded in TCNQI$_2$ (or the thermal motions are less). The exocyclic C≡C bond is the same in the parent and in TCNQI$_2$. The average of the C$_2$–C$_4$ bond lengths is 0.007 Å shorter in TCNQI$_2$ than in TCNQ. The C$_3$C$_2$C$_3'$ angle is 2° smaller in TCNQI$_2$, but the C$_1$C$_3$C$_3'$ bond angle is increased by 3°. Surprisingly, the C$_1$C$_3'$C$_3$ bond angle is only 0.8° smaller than the same angle in TCNQ even though the I is bonded at the central carbon. The biggest difference between TCNQ and TCNQI$_2$ is found for the C$_2$C$_4$N' bond angle which is adjacent to the I. Whereas the CCN bonds are essentially linear in TCNQ, they are 10° away from linearity for [TCNQI$_2$]$^{\bullet-}$. The cyano group bends away from the I presumably due to its large steric bulk. Consistent with this deviation in the CCN bond angle is the decrease in the C$_4$C$_2$C$_4'$ angle in TCNQI$_2$ by almost 6° as compared to TCNQ.[22] The C(CN)$_2$ group also rocks away from the I with C$_3'$C$_1$C$_2$ = 126.6° and C$_3$C$_1$C$_2$ = 117.2°. The C≡N group also rocks away from the I with C$_1$C$_2$C$_4'$ and C$_1$C$_2$C$_4$ angles of 128.5° and 121.1°, respectively.

[Fe(C$_5$Me$_5$)$_2$]$^{\bullet+}$[TCNQI$_2$]$^{\bullet-}$. The monoclinic unit cell is comprised of unique cations and anions. Anion atom labeling, bond distances, and angles for the anion are given in Figure 1 and are summarized in Table III. Atom labeling for the cation can be found in Figure S2.

[Fe(C$_5$Me$_5$)$_2$]$^{\bullet+}$. The C$_5$ rings are rotated by 4° away from ideal D_{5h} symmetry for the [Fe(C$_5$)$_2$]$^{\bullet+}$ moiety. The Fe–C, C–C, and C–Me bond distances range from 2.095 (6)–2.121 (6), 1.417 (8)–1.438 (8), and 1.490 (8)–1.500 (9) Å, respectively, and average 2.106, 1.429, and 1.496 Å, respectively. These values are in good agreement with other reported structures.[9a] The Fe–C$_5$ ring centroids average 1.720 Å and are slightly longer (0.02 Å) than those previously reported.[9b]

[TCNQI$_2$]$^{\bullet-}$'s structure is reported for the first time. The structure of [TCNQI$_2$]$^{\bullet-}$ is nonplanar, Figure 1, in contrast to the structure found for [TCNQ]$^{\bullet-}$ even though the radical anions in both structures are sandwiched between parallel C$_5$ rings on two adjacent intrachain cations in an ···D$^{\bullet+}$A$^{\bullet-}$D$^{\bullet+}$A$^{\bullet-}$D$^{\bullet+}$A$^{\bullet-}$··· arrangement. The C(CN)$_2$ groups rotate by 9° and 16° in opposite directions to give the ion an approximate center of inversion. The average C$_3$–C$_3'$ distance is comparable to that in TCNQI$_2$. The remaining C–C ring distances in the ion are shorter than in TCNQI$_2$ in agreement with the expectation of increased aromatic character in the ring. The exocyclic C$_1$–C$_2$ bonds are longer in

(22) Long, R. E.; Sparks, R. A.; Trueblood, K. N. *Acta Crystallogr.* **1965**, *18*, 932.

Table III. Calculated or Observed Bond Distances, Å, and Angles, deg, for TCNQI₂, [TCNQI₂]·⁻, and [TCNQI₂]²⁻

parameter	TCNQI₂ (C₂ₕ) obs	TCNQI₂ (C₂ₕ) calc	[TCNQI₂]·⁻ (Cᵢ) obs^a	[TCNQI₂]²⁻ (Cᵢ) obs	[TCNQI₂]²⁻ (Cᵢ) calc	[TCNQIᵢ]²⁻ (C₂ₕ) calc
C₁-C₂	1.388 (2)	1.354	1.409 (9)	1.458 (8)	1.473	1.469
C₁-C₃	1.445 (2)	1.487	1.428 (8)	1.384 (8)	1.408	1.409
C₁-C₃'	1.449 (2)	1.495	1.438 (8)	1.411 (8)	1.412	1.414
C₂-C₄	1.440 (3)	1.463	1.425 (10)	1.408 (8)	1.418	1.422
C₂-C₄'	1.430 (3)	1.459	1.420 (9)	1.411 (8)	1.416	1.416
C₃-C₃'	1.356 (3)	1.332	1.348 (9)	1.384 (8)	1.387	1.386
C₄-N	1.148 (3)	1.158	1.143 (9)	1.125 (8)	1.164	1.163
C₄'-N'	1.139 (3)	1.159	1.145 (8)	1.149 (8)	1.164	1.164
C₃-H	1.010 (27)	1.082			1.080	1.079
C₃'-I	2.080 (2)	2.084	2.102 (6)	2.095 (8)	2.119	2.120
C₃C₁C₃'	116.7 (2)	115.0	113.8 (6)	114.0 (5)	113.4	112.7
C₂C₁C₃	117.2 (2)	117.4	118.3 (6)	119.4 (5)	118.8	118.0
C₂C₁C₃'	126.0 (2)	127.6	128.0 (6)	126.6 (5)	127.8	129.2
C₁C₂C₄	120.3 (2)	120.9	118.3 (6)	114.4 (5)	119.3	119.3
C₁C₂C₄'	128.8 (2)	128.4	129.8 (6)	127.0 (6)	125.2	127.4
C₄C₂C₄'	110.9 (2)	110.7	111.7 (6)	117.9 (5)	114.8	113.3
C₁C₃C₃'	123.4 (2)	126.2	124.7 (6)	123.4 (5)	124.8	125.5
C₁C₃'C₃	119.8 (2)	118.9	121.6 (6)	122.5 (5)	121.8	121.7
C₁C₃H	113. (1)	114.9			116.8	116.4
C₃'C₃H	123. (1)	118.9			118.4	118.1
C₁C₃'I	124.4 (1)	124.0	122.8 (5)	122.0 (5)	122.9	124.1
C₃C₃'I	115.7 (1)	117.1	115.5 (5)	115.3 (4)	115.2	114.2
C₂C₄N	177.4 (3)	178.8	178.8 (8)	174.3 (7)	178.4	178.6
C₂C₄'N'	169.8 (2)	172.9	171.6 (9)	174.9 (7)	175.2	173.9

^a Average of two values. The structure has approximate Cᵢ symmetry.

the ion by 0.03 Å consistent with the loss of double bond character. The C₂-C₄ and C₂-C₄' bonds decrease by 0.012 and 0.009 Å, respectively, in the ion consistent with delocalization of negative charge to the cyano groups. The C-I bonds are 0.025 Å longer in the anion suggesting some anionic hyperconjugation by I. The C₃C₁C₃' bond angles decrease in the anion as compared to the neutral. The other internal ring angles increase somewhat in the anion. Since the anion is nonplanar, the angle C₄C₂C₄' can increase by 1.2°. However the rock of the C(CN)₂ group [θ(C₁C₂C₄')] away from the I is even more pronounced in the anion. The CCN bond angles [θ(C₂C₄'N')] adjacent to the I still deviate from linearity by 8°.

Solid-State Structure. Analogous to the structures the [Fe-(C₅Me₅)₂]·⁺ salts of [DDQ]·⁻,[10a] [TCNQ]·⁻,[17] [TCNE]·⁻,[9] [C₃-(CN)₅]⁻,[9a] {Ni[S₂C₂(CF₃)₂]₂}·⁻,[11] and [C₄(CN)₆]·⁻,[12] [Fe-(C₅Me₄H)₂]·⁺[TCNE]·⁻,[24] and [Fe(C₅Me₄H)₂]·⁺[TCNQ]·⁻[24] the radical anion is sandwiched between parallel C₅ rings on two adjacent intrachain cations in an ···D·⁺A·⁻D·⁺A·⁻D·⁺A·⁻··· arrangement, Figures 2 and 3. Unlike these other substances, however, the Cₛ anion in this structure is significantly nonplanar. As noted in Table IV the intrachain Fe···Fe distance is 11.131 (2) Å, 0.58 Å longer than observed for metamagnetic [Fe-(C₅Me₅)₂]·⁺[TCNQ]·⁻,[17] 0.61 Å longer than that observed for the bulk ferromagnet (orthorhombic) [Fe(C₅Me₅)₂]·⁺[TCNE]·⁻,[9a] and 0.37 Å longer than in ferromagnetically coupled [Fe-(C₅Me₅)₂]·⁺[C₄(CN)₆]·⁻.[12] The distance is also longer than that observed for the similarly structured paramagnetic complexes, i.e., the [C₃(CN)₅]⁻,[9a] [DDQ]·⁻,[10a] and {C₃[C(CN)₂]₃}·⁻[25] salts. One possibility for the increased distance is the bulk of the iodine. Although the ···D·⁺A·⁻D·⁺A·⁻··· chains are parallel to the a-axis, the C₅ ring of the cation and the C₆ ring of the anion are tipped 19.0° with respect to a, and there is a 2.09 Å displacement from one D·⁺ or A·⁻ to another.
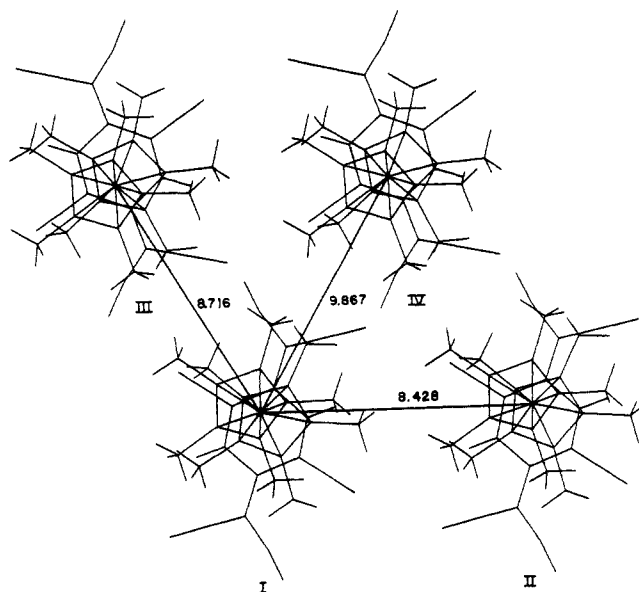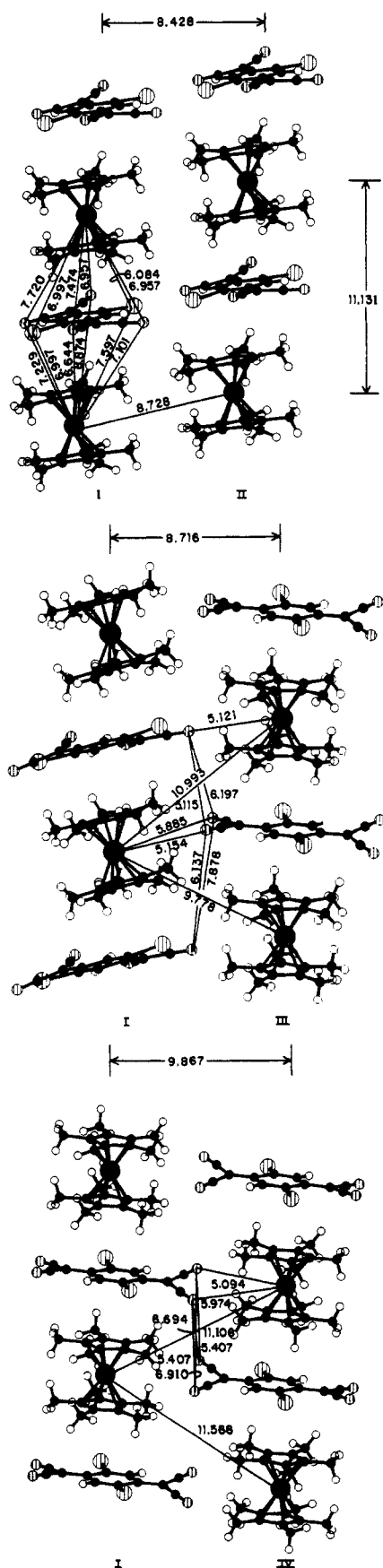
(23) Miller, J. S.; Zhang, J. H.; Reiff, W. M.; Preston, L. D.; Reis, A. H., Jr.; Gebert, E.; Extine, M.; Troup, J.; Dixon, D. A.; Epstein, A. J.; Ward, M. D. *J. Phys. Chem.* **1987**, *91*, 4344.

(24) Miller, J. S.; Glatzhofer, D. T.; O'Hare, D. M.; Reiff, W. M.; Chakraborty, A.; Epstein, A. J. *Inorg. Chem.* **1989**, *28*, 2930.

Figure 2. View down the 1-D chains of [Fe(C₅Me₅)₂]·⁺[TCNQI₂]·⁻ showing the unique chains, I-IV.

Since ferromagnetism is a bulk property, the intrachain as well as the interchain interactions are of fundamental importance. This information is important to understand the spin-spin interactions which should dominate the magnetic behavior. The various inter- and intrachain Fe···Fe, Fe···N, and N···N separations are given in Table IV. The unit cell has three unique interchain interactions, namely I and II, I and III, and I and IV, Figure 2. Chains I and II are essentially in-registry, Figure 3a, whereas chains I and III and I and IV are out-of-registry, Figure 3b and c.

The intrachain Fe···N interactions, Figure 3a, range from 6.64 to 8.87 Å and are comparable to those reported for the similarly structured [TCNQ]·⁻ and [TCNE]·⁻ salts. The intrachain Fe···I interactions, Figure 3a, range from 6.08 to 7.72 Å. The shortest

5500 *J. Am. Chem. Soc., Vol. 112, No. 14, 1990*

Miller et al.

Figure 3. In-registry interactions between chains I and II (a) and out-of-registry interactions between chains 1 and III (b) and I and IV (c).
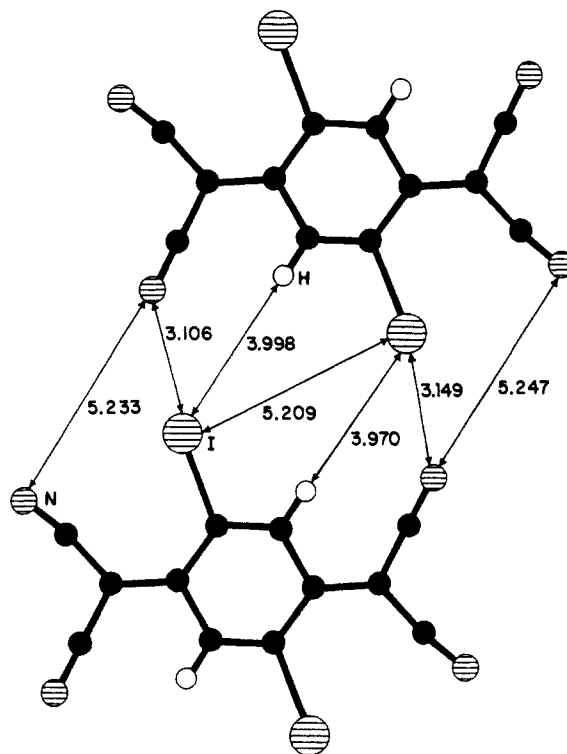
Figure 4. In-registry [TCNQI₂]·⁻···[TCNQI₂]·⁻ distances.

to the comparable in-registry distances observed for the ferro-magnetically coupled [TCNE]·⁻ ⁹ and [C₄(CN)₆]·⁻ ¹² salts, Table IV. The Fe···Fe distance is 0.3 Å greater than the I and II separation normal to the chains. For the out-of-registry chain interactions the Fe···Fe separations are 9.78, 10.99, 11.11, and 11.57 Å. Although these values are 0.3–0.5 Å longer than those in similarly structured salts, the [TCNQI₂]·⁻ salt exhibits tilting of the chains and a rotation of the anion. In contrast the out-of-registry Fe···N spacings are typically shorter, Table IV.

The in-registry anion/anion interactions could be important for antiferromagnetic behavior. The [TCNQI₂]·⁻/[TCNQI₂]·⁻ interaction, Figure 4, is significantly different to those observed for the [TCNE]·⁻,⁹ᵃ [TCNQ]·⁻,²³ [DDQ]·⁻,¹⁰ᵃ and [C₄(CN)₆]·⁻ ¹² salts, Table IV. The shortest in-registry N···N distance is 5.23 Å, Figure 4, and is substantially longer than observed for the monoclinic phase of the [TCNE]·⁻ salt (i.e., >0.5 Å) and 1.3 Å longer than that observed for the metamagnetic [TCNQ]·⁻ salt. Additionally, the [TCNQI₂]·⁻ salt has short N···I spacings of 3.11 and 3.15 Å. Even though the C≡N···I interactions are not linear, they are ~0.6 Å shorter than the sum of the van der Waals radii.²⁶ In comparison to the metamagnetic [TCNQ]·⁻ salt the closest N···HC interactions are 2.53 and 2.78 Å which is comparable to the sum of the van der Waals radii.²⁶

{[Co(C₅Me₅)₂]·⁺}₂[TCNQI₂]²⁻. The triclinic unit cell is comprised of a unique cation and one-half of an anion. Dianion atom designations, bond distances, and angles are located in Table III, respectively. Atom labeling for the cation and anion can be found in Figure S3.

[Co(C₅Me₅)₂]·⁺. The C₅ rings are staggered giving the cation *D*₅*d* symmetry for the [Co(C₅)₂]·⁺ moiety. The Co–C, C–C, and C–Me bond distances range from 2.035 (6)–2.057 (6), 1.414 (9)–1.449 (9), and 1.485 (8)–1.508 (8) Å, respectively, and average 2.046, 1.426, and 1.494 Å, respectively. These values are in good agreement with other reported structures for the cation, and the Co–C distances are ~0.04 Å shorter than the comparable Fe–C distances observed for [Fe(C₅Me₅)₂]·⁺.²³,²⁵,²⁷,²⁸ The distance from the Co to the C₅ ring centroid is 1.650 Å in excellent

interchain Fe···Fe, Fe···N, and N···N separations for the in-registry I and II chains are 8.73, 7.70, and 5.23 Å, respectively. The in-registry Fe···Fe separation is essentially equivalent (±0.1 Å)

(25) Miller, J. S.; Ward, M. D.; Zhang, J.; Reiff, W. M. Manuscript in preparation.

(26) Pauling, L. *The Nature of the Chemical Bond*, 3rd ed.; Cornell University Press: Ithaca, NY, 1960.

Table IV. Summary of the Intra- and Interchain Fe···Fe, Fe···N, and N···N Interactions for [Fe(C₅Me₅)₂]•⁺[anion]•⁻ Possessing the ···D•⁺A•⁻D•⁺A•⁻··· Structure

[anion]•⁻, [A]•⁻	[TCNE]•⁻ monoclinic	[TCNE]•⁻ orthorhombic	[TCNQ]•⁻	[TCNQI₂]•⁻	[C₄(CN)₆]•⁻	[DDQ]•⁻
separation						
Fe···Fe, Å interchain	10.415	10.621	10.549	11.131	10.783	10.616
Fe···Fe, Å in-registry	8.732	8.689	8.628	8.728	8.719	8.692
Fe···Fe, Å out-of-registry	9.473	9.618	9.384	9.778	9.865	9.723
	10.028	9.649	10.670	10.993	10.030	10.033
N···N, Å	4.721		3.922	5.236	3.311	7.006
	6.587		5.308	5.253	3.939	
				5.407		
Fe···N, Å	5.670		5.249	5.094	5.153	5.369
	5.707		5.451	5.121		
			5.829	5.154	5.856	5.501
				5.885		
				5.974		
ref	8a	8a	17	this work	11	10a

agreement with previously reported values.[23,25,27,28]

[TCNQI₂]²⁻'s structure is reported for the first time. The structure of [TCNQI₂]²⁻ is nonplanar with twisting about the C₁–C₂ bonds of 26° to give an ion of Cᵢ symmetry, i.e., the planes containing the cyano groups are rotated in the same direction. The rotation of the planes about the C₁–C₂ bonds is an average value, and the actual values for the τ(C₃C₁C₂C₄′) and τ-(C₃′C₁C₂C₄) torsion angles are 31° and 21° showing that the CN group adjacent to I is rotated further out of the plane. The C₁–C₂ torsions are larger in the dianion (26°) than in either [TCNQ]•⁻ (12°) or TCNQI₂ (4°). The nonplanarity of [TCNQI₂]²⁻ is in contrast to the planar structure found for [TCNQ]²⁻ even though the dianions in both structures are sandwiched between parallel C₅ rings on two adjacent intrachain cations in a ··· D⁺D⁺A²⁻D⁺D⁺A²⁻D⁺D⁺A²⁻··· arrangement. Thus, the packing does not effect the inherent structure of the dianion. The differences in the structure of TCNQI₂ and [TCNQI₂]²⁻ are as expected. The C₁–C₂ bond lengthens as compared to the n = 0 and n = 1– structures to a value more like that of a C–C single bond. The C–C ring bonds become more equal for [TCNQI₂]²⁻ although the C₃–C₃′ bond is still the shortest value. The C₂–C₄ and C₂–C₄′ bonds clearly decrease in the dianion consistent with delocalization of negative charge to the cyano groups. The C–I bonds in [TCNQI₂]²⁻ are comparable to those in [TCNQI₂]•⁻. The angles at C₂ change as charge is added with the angle C₄C₂C₄′ increasing as steric interactions of the CN group and the I are relieved by twisting about the C₁–C₂ bond and as more C=C character is found in the C₂–C₄ and C₂–C₄′ bonds. The increased torsion about the C₁–C₂ bond leads to decreased steric interactions between the CN and the I, enabling the C₂C₄′N′ angle to become more linear. However, the increased charge on the cyano groups causes the angle θ(C₂C₄N) to become more nonlinear.

Solid-State Structure. Similar to the structures of the 2:1 [Fe(C₅Me₅)₂]•⁺ salts of [C₄(CN)₆]²⁻[28] and [TCNQF₄]²⁻,[29] the dianion is sandwiched between parallel C₅ rings on two adjacent intrachain cations in an ···D⁺A²⁻D⁺D⁺A²⁻D⁺··· arrangement along the 1̄11 crystallographic direction, Figure 5. Unlike the [DDQ]²⁻, [TCNQ]²⁻, and [C₄(CN)₆]²⁻ salts, the [TCNQI₂]²⁻ as discussed above is significantly nonplanar. A similar nonplanarity is observed for the [TCNQF₄]²⁻ salt.[29] There are no short N···I contacts present in this structure.

The intrachain Co···Co separations are 7.148 and 10.667 Å, whereas the intrachain separations below 10 Å are 8.88, 9.15, 9.29,
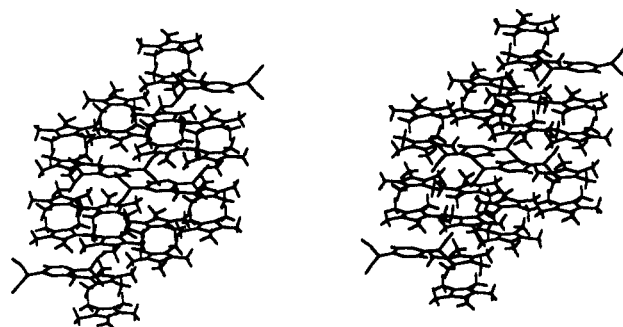

Figure 5. Stereoview of the unit cell of {[Co(C₅Me₅)₂]•⁺}₂[TCNQI₂]²⁻.

9.32, 9.54, and 9.88 Å. The parallel chains are separated by 8.48, 8.98, 9.06, and 9.64 Å. The intrachain Co···Co separations are comparable to the 7.08 and 10.63 Å observed for {[Fe-(C₅Me₅)₂]•⁺}₂[C₄(CN)₆]²⁻.[33] Due to the lack of colinearity for the 1-D chains in {[Fe(C₅Me₅)₂]•⁺}₂[TCNQF₄]²⁻,[29] the D⁺D⁺ Fe···Fe separation in the [TCNQF₄]²⁻ salt is substantially greater (9.17 Å) than the value observed for the [TCNQI₂]²⁻ salt (7.15 Å). The D⁺A²⁻D⁺ Fe···Fe separations are, however, comparable (10.49 vs 10.68 Å).

Molecular Orbital Theory Structural Results. The calculated geometry parameters for planar TCNQI₂ and [TCNQI₂]²⁻ are given in Table III. The planar TCNQI₂ is not a minimum at the SCF level but is a transition state characterized by one negative degree of curvature (an imaginary frequency of 15i cm⁻¹). This motion breaks the molecular plane leading to a boat shaped structure that is 1.0 kcal/mol more stable at the SCF level. Inclusion of a correlation correction reverses the energy ordering making the C₂ₕ structure more stable by 1.0 kcal/mol in agreement with the crystal structure result. Thus the surface for folding the molecule is very flat, and we compare the experimental and calculated planar structures. The C=C bond distances are calculated to be too short by 0.02–0.03 Å, whereas the C–C bonds are calculated to be too long by 0.03–0.04 Å. The C≡N bonds are calculated to be too long by ~0.02 Å. The calculated and observed C–I bond distances are in very good agreement. Considering the differences in the bond lengths, the calculated bond angles are in good agreement with the experimental values. The calculations reproduce the large steric interaction of the I with C(CN)₂ properly including the nonlinearity of the CCN bond adjacent to the I, although the experimental bond angle is 3° larger. The differences between theory and experiment are very similar to our previous calculations on [TCNQ]ⁿ[23] and [TCNQF₄]ⁿ.[29] The folded structure, Figure 6 (see supplementary material for coordinates and geometry parameters), is similar to the planar structure with the C–C ring bond distances ~0.005

(27) (a) Miller, J. S.; Dixon, D. A. *Science* **1987**, *235*, 871. (b) Dixon, D. A.; Miller, J. S. *J. Am. Chem. Soc.* **1987**, *109*, 3656.

(28) Miller, J. S.; Calabrese, J. C.; Dixon, D. A. Manuscript in preparation.

(29) Dixon, D. A.; Calabrese, J. C.; Miller, J. S. *J. Phys. Chem.* **1989**, *93*, 2284.

5502 *J. Am. Chem. Soc., Vol. 112, No. 14, 1990*

Miller et al.

Table V. Charges and Spins for [TCNQI$_2$]$^{n-}$ (n = 0, 1, 2)

| atom | charges for [TCNQI$_2$]$^{n-}$ | | | spin for [TCNQI$_2$]$^-$ | | | |
	$n = 0$	$n = 1$	$n = 2$	total	p$_z$	s	p$_x$ + p$_y$
C$_1$	0.05	-0.01	0.01	-0.27	-0.17	-0.04	-0.06
C$_2$	0.02	-0.03	-0.18	0.71	0.46	0.10	0.15
C$_3$	-0.05	-0.07	-0.09	0.13	0.09	0.02	0.02
C$_3'$	-0.07	-0.10	-0.10	-0.03	-0.02	0.00	0.00
C$_4$	0.07	0.07	0.04	-0.77	-0.32	-0.11	-0.34
C$_4'$	0.08	0.06	0.04	-0.82	-0.34	-0.11	-0.37
N	-0.16	-0.23	-0.36	0.75	0.39	0.04	0.32
N'	-0.15	-0.22	-0.35	0.80	0.41	0.04	0.35
H	0.10	0.06	0.05	-0.01	0.00	-0.01	0.00
I	0.13	-0.02	-0.07	0.00	0.00	0.00	0.00

Table VI. Experimental IR $\nu_{C\equiv N}$ Frequencies for [TCNQI$_2$]$^{n-}$

	$\nu_{C\equiv N}$, cm^{-1}
TCNQI$_2$	2214, 2201
[Fe(C$_5$Me$_5$)$_2$]$^{·+}$[TCNQI$_2$]$^{·-}$	2180, 2149
[Co(C$_5$Me$_5$)$_2$]$^+$[TCNQI$_2$]$^{·-}$	2180, 2150
{[Co(C$_5$Me$_5$)$_2$]$^+$}$_2$[TCNQI$_2$]$^{2-}$	2180 w, 2113 s, 2156 s, 2180 w
[TCNQ(OMe)$_2$]$^{·-}$	2201, 2191, 2169
[TCNQMe$_2$]$^{·-}$	2197, 2189, 2173, 2156
[TCNQCl$_2$]$^{·-}$	2189, 2184, 2162
[TCNQBr$_2$]$^{·-}$	2187, 2181, 2156

A longer and the C=C bonds slightly shorter due to the small loss of delocalization. The C–CN and C≡N bonds do not show significant changes on folding except that the CCN bond angle adjacent to the I gets 1° closer to linearity.

The force field calculations on the planar dianion show two imaginary frequencies of 22i and 23i cm^{-1} which correspond to the asymmetric (a$_u$) and symmetric (b$_g$) coupling of the twists about the C$_1$–C$_2$ bonds. Following the larger curvature led to the symmetric twist with both C(CN)$_2$ planes rotated in the same direction to give a structure of C$_i$ symmetry in agreement with the crystal structure. The calculated torsion angles about the C$_1$–C$_2$ bonds are 21° for rotation of the CN group adjacent to the H and 31° for rotation of the CN group adjacent to I which are the same as the experimental torsions. At the SCF level, the C$_i$ structure is 0.7 kcal/mol lower in energy than the planar C$_{2h}$ structure. Correlation corrections may favor the planar structure (an MP-2 calculation places the planar structure 0.7 kcal/mol below the C$_i$ structure), but the basis set is not adequate enough to distinguish between the C$_i$ and C$_{2h}$ structures at a correlated level. The important feature is that the potential energy surface for torsion about the C$_1$–C$_2$ bond is very flat although the lowest energy deformation mode is now this torsion rather than the folding of the ring found for TCNQI$_2$. The agreement of the calculated bond lengths with the experimental values is quite good with the calculated values excluding r(C≡N) being 0.001–0.024 Å too long. The calculated angles are in reasonable agreement with the experimental values. The largest differences are in the angles at C$_2$ where the calculated value for θ(C$_4$C$_2$C$_4$) is 3° smaller than the experimental value whereas θ(C$_1$C$_2$C$_4$) is calculated to be 5° larger than the experimental value. The other difference is found for θ(C$_2$C$_4$N) where the calculated value is more nearly linear.

The calculated geometry of the planar dianion can be compared to the planar TCNQI$_2$ structure. The C$_1$–C$_2$ and C$_3$–C$_3'$ bonds increase; whereas the C$_1$–C$_3$ and C$_1$–C$_3'$ ring bonds decrease in length. The changes are those expected as the ring approaches an aromatic system as expected from simple valence bond considerations. The C–I bond lengthens by 0.044 Å as the two negative charges are added. The differences between TCNQI$_2$ and [TCNQI$_2$]$^{2-}$ are essentially the same as those calculated for the neutral and dianion of TCNQ[23] and TCNQF$_4$.[29]

Charge and Spin Distributions. The Mulliken charges are given in Table V. The charges in TCNQI$_2$ are essentially the same as those in TCNQ[23] with the N bearing the largest negative charge and the C–H and C–I bond polarized δ^-/δ^+. Addition of a negative charge leads to a further accumulation of negative charge on the nitrogens and in the C$_1$–C$_2$ region. There is also some accumulation of negative charge on the I. In the dianion, the nitrogens bear the largest negative charges followed by the C$_1$–C$_2$ bond region. The C–I bonds gain some negative charge but not as much as seen in going from the TCNQI$_2$ to the [TCNQI$_2$]$^{·-}$. The C$_1$–C$_2$, C$_2$–C$_{4(4')}$, and C≡N bonds have significantly increased their polarity in the dianion with the C–I bond becoming almost nonpolar.

The spin population, Table V, is calculated within the UHF framework and is defined as the difference in the Mulliken populations for the α and β electrons. Positive spin implies an

excess of α electrons and negative spin implies an excess of β electrons (α = β + 1). The largest α spin is predicted to be on the nitrogens with an almost identical excess α spin on C$_2$. The largest negative spins are predicted to be on the carbons bonded to the nitrogens. There is essentially no spin in the C$_3'$–I region even though there is spin on C$_3$. Thus, there is likely to be little spin transfer from the C–I region to an adjacent ion. The spin on the atoms carrying large spins is about equally divided between the in- and out-of-plane components for C$_4$ and N. The out-of-plane spin is dominant on C$_1$, C$_2$, and C$_3$. The EPR behavior is governed by the interactions of the electron spins in the s orbitals with the nuclear spins. The largest ^{13}C hyperfine splitting is expected to be at C$_4$ and C$_4'$ with the coupling constant at C$_2$ being of comparable magnitude but of opposite sign. The coupling constant at C$_1$ is smaller and is the same sign as those on C$_4$ and C$_4'$. The 2s population on N is of the same size as that for C$_1$, but the coupling constant would be of opposite sign. These results are very similar to those found for [TCNQ]$^{·-}$[23] and [TCNQF$_4$]$^{·-}$.[29]

Observed Spectroscopic Properties. The $\nu_{C\equiv N}$ are summarized in Table VI. There are two $\nu_{C\equiv N}$ stretches in the IR for TCNQI$_2$. The C≡N stretches in TCNQI$_2$ are red shifted as compared to their values in TCNQ[23] and TCNQF$_4$.[29] The asymmetric C=C stretches at 1497 and 1520 cm^{-1} in TCNQI$_2$ are also red-shifed from the values of 1540 and 1545 cm^{-1} found for TCNQ[23] and are significantly red-shifted from the values of 1574 and 1601 cm^{-1} in TCNQF$_4$.[29] [TCNQI$_2$]$^{·-}$ has the same $\nu_{C\equiv N}$ stretching transitions for either salt which are red-shifted from TCNQI$_2$ and are split by 30 cm^{-1}. The cyano stretches are very similar to the values in [TCNQ]$^{·-}$[23] and are red-shifted from the values in [TCNQF$_4$]$^{·-}$.[29] The cyano stretches for [TCNQI$_2$]$^{2-}$ show four peaks; two intense absorptions (2113 and 2156 cm^{-1}) each of which shows a weak shoulder (2080 and 2179 cm^{-1}). The shift of the cyano stretches to lower frequency combined with an increased splitting is a signature for the formation of the dianion. For example, the two IR peaks in [TCNQ]$^{·-}$ are at 2105 and 2150 cm^{-1},[23] whereas in [TCNQF$_4$]$^{·-}$ the two peaks are at 2133 and 2167 cm^{-1}.[29]

The other disubstituted structures also show characteristic IR spectra for their monoanion salts. The spectra of [TCNQBr$_2$]$^{·-}$ and [TCNQCl$_2$]$^{·-}$ show a split high-frequency band and a single lower frequency band. The bands are slightly blue-shifted as compared to [TCNQI$_2$]$^{·-}$. The spectra for [TCNQMe$_2$]$^{·-}$ and [TCNQ(OMe)$_2$]$^{·-}$ salts behave quite differently. In the other compounds studied, the base line is reasonably flat, and the cyano stretches are sharp and moderately intense for the anion salts. For the two latter compounds, the base line dispersion is present with the absorption increasing with increasing frequency. This is consistent with the presence of metal-like or semiconducting chains of [TCNQR$_2$]$^{·-}$. Also, the $\nu_{C\equiv N}$ stretches are quite weak and broad. For the OMe derivative, the two most intense peaks are at 2169 and 2191 cm^{-1} with a shoulder at 2201 cm^{-1} on the higher frequency peak. For the Me derivative, the high field peak is at 2189 cm^{-1} with a 2197-cm^{-1} shoulder. The lower frequency peak is at 2173 cm^{-1} with a broad peak at 2156 cm^{-1}. Furthermore, there is an additional broad peak at 2122 cm^{-1}. The spectra of these compounds are consistent with the presence of the mononoanion, but other absorption effects are also occurring. The actual symmetry for the Me and OMe derivatives are likely to be lower due to the presence of the methyl groups.

The UV–visible spectra of [TCNQI$_2$]$^{n-}$ (n = 0, 1, 2) are essentially the same as that found in [TCNQ]$^{n-}$[23] and

Decamethylferrocene Electron-Transfer Salts

J. Am. Chem. Soc., Vol. 112, No. 14, 1990 5503

Table VII. Electronic Absorption Spectral Parameters for $TCNQI_2$, $[TCNQI_2]^-$, and $[TCNQI_2]^{2-}$

absorption maxima		molar extinction,
λ_{max}, nm	λ_{max}, cm^{-1}	ϵ, cm^{-1} M^{-1}
$TCNQI_2$		
412	24 275	36 775
330 sh	30 300	4 125
222	45 050	9 210
$[TCNQI_2]^{-a}$		
874	11 440	27 675
782	12 790	13 900
770	12 990	13 925
700 sh	14 290	4 230
432	23 150	16 310
404 sh	24 750	14 230
292	34 250	40 000
234	42 735	16 250
$[TCNQI_2]^{2-a}$		
304	32 895	18 900
293	34 130	55 400
231	43 300	21 650

^{a} As the $[Co(C_5Me_5)_2]^+$ salts.

$[TCNQF_4]^{-}$.[29] The λ_{max} and molar extinction coefficients, ϵ, are summarized in Table VII. The analysis of these spectra has been discussed in detail previously and will not be discussed here.

Calculated Spectroscopic Properties. The calculated harmonic frequencies for the C_{2h} structure of $TCNQI_2$ and C_{2h} and C_i structures of $[TCNQI_2]^{2-}$ are given in Table VIII. The force fields show that there is one imaginary frequency for planar $TCNQI_2$ and two for planar $[TCNQI_2]^{2-}$ as discussed previously. The imaginary frequencies correspond to low-energy out-of-plane modes. Upon folding of $TCNQI_2$ the imaginary frequency becomes real with a small value. The remaining frequencies show shifts of at most 20–30 cm^{-1}. For $[TCNQI_2]^{2-}$, twisting about the C_1–C_2 bonds converts the two imaginary frequencies into real frequencies at 24 and 29 cm^{-1} with the remaining frequencies only showing small changes. Thus, we focus on the force fields for the planar structures since this is appropriate for comparison to $TCNQI_2$ and because the transitions break into symmetry blocks. We note that the a_g and b_g frequencies are IR inactive due to symmetry. However, for accidently degenerate orbitals, there is some intensity in the a_g transitions borrowed from the b_u transitions. A similar feature is observed for the C_i structure. For $TCNQI_2$, this is found in the C–H and C≡N stretches. There is also one lower frequency vibration for each structure. The infrared intensities are only meant to provide qualitative information in the spirit of the spectroscopist's strong, medium, or weak notation.

The calculated frequencies are too large in comparison to the experimental values. This is due to the use of a small basis set where correlation effects and anharmonic corrections are neglected. These effects can be accounted for by scaling the calculated frequencies. Previously, the scale factor of 0.82 was determined to be appropriate for the C—H, C≡N, and C═C stretches in TCNQ and a scale factor of 0.9 for the remaining frequencies.[23] Table VIII compares the calculated scaled frequencies to experiment. The scaled IR active C≡N stretches are high by ~15 cm^{-1} for $TCNQI_2$ and are high by a comparable amount for $[TCNQI_2]^{2-}$. For the C═C stretches a scale factor of 0.79 is more appropriate in agreement with our calculations on $[TCNQF_4]^n$.[29] The calculations show that the IR transitions for the dianion are expected to be significantly more intense than for $TCNQI_2$ in agreement with our previous work on $TCNQ^{23}$ and $TCNQF_4$.[29] The increased charge separation in the dianion leads to increased dipole moment derivatives and increased intensities. The transitions corresponding to the C≡N and C═C stretches are all predicted to be quite intense in $[TCNQI_2]^{2-}$.

^{57}Fe Mössbauer Spectroscopy. The temperature dependence of the ^{57}Fe Mössbauer spectra of $[Fe(C_5Me_5)_2]^{\bullet+}[TCNQI_2]^{\bullet-}$ was
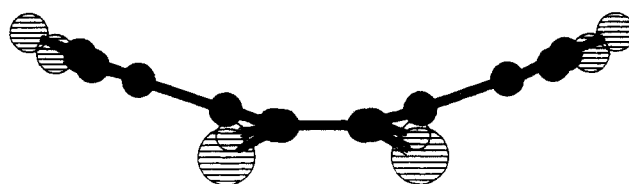
Figure 6. Folded $[TCNQI_2]^{\bullet-}$ structure.
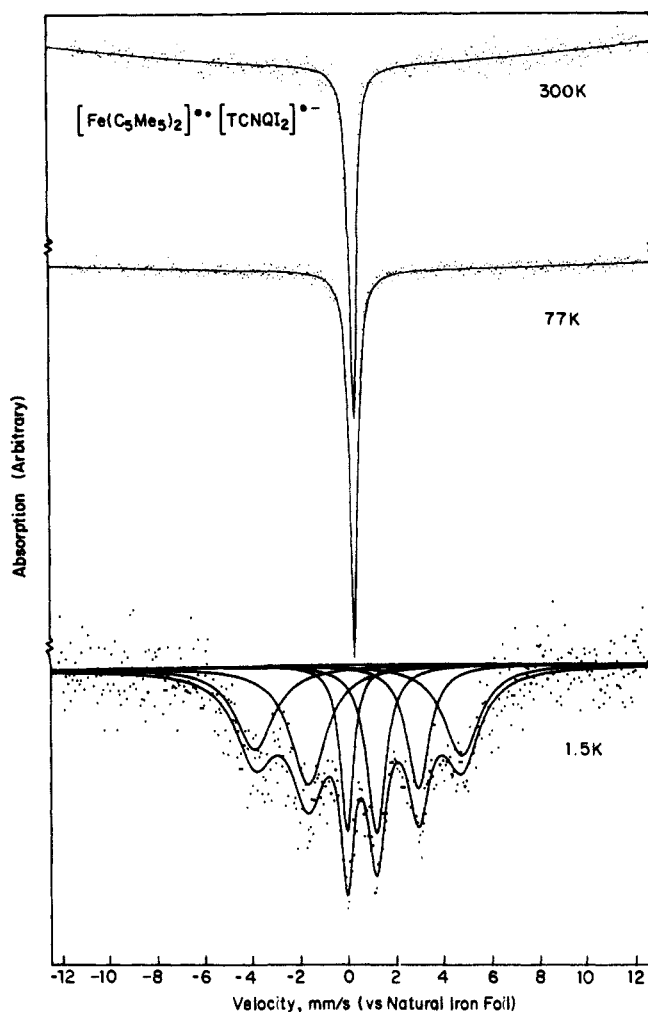
Figure 7. ^{57}Fe Mössbauer spectra of $[Fe(C_5Me_5)_2]^{\bullet+}[TCNQI_2]^{\bullet-}$.

obtained between 1.5 and 300 K. For the decamethylferrocenium salt, a relatively narrow line width singlet characteristic of low-spin Fe^{III} [30] was observed [isomer shift, δ (line width, Γ) 0.474 (0.367) and 0.528 mm/s (0.388 mm/s) at 300 and 77 K, respectively, Figure 7 top and middle]. This singlet is broadened at 4.2 K, while at 1.50 K a partially resolved hyperfine split spectrum is observed corresponding to an internal field of 270 kG (27 T). The large increase in internal hyperfine field suggests incipient magnetic ordering with a critical temperature below 4.2 K.

It is worthwhile to compare the behavior of $[Fe(C_5Me_5)_2]^{\bullet+}[TCNQI_2]^{\bullet-}$ with those of other well characterized salts of $[Fe(C_5Me_5)_2]^{\bullet+}$. There are two extremes of behavior, namely slow paramagnetic relaxation, as evidenced by the gradual onset of magnetic hyperfine splitting for which the corresponding internal hyperfine field, H_n is relatively temperature independent, and 3-D magnetic order which generally occurs more suddenly over a small temperature range and for which dH_n/dT is large near T_c. $[Fe(C_5Me_5)_2]^{\bullet+}[TCNE]^{\bullet-9a}$ and $[Fe(C_5Me_5)_2]^{\bullet+}[C_4-(CN)_6]^{\bullet-12}$ are excellent examples of the latter behavior. $[Fe(C_5Me_5)_2]^{\bullet+}[TCNQI_2]^{\bullet-}$ is clearly more reminiscent of the latter behavior except that magnetic saturation and a limiting value of H_n typically ~440 kG are not achieved at the lowest temperature, ~1.5 K, measured.
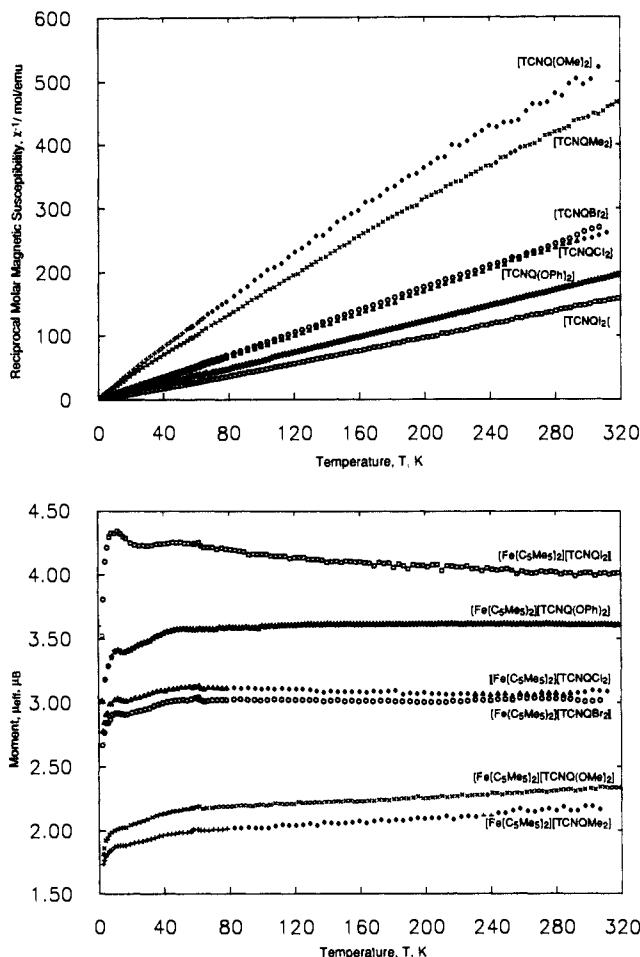
Table VIII. Calculated Vibrational Frequencies for TCNQI₂ and [TCNQI₂]²⁻

symmetry	TCNQI₂ (C₂ₕ)			[TCNQI₂]²⁻ (C₂ₕ)			[TCNQI₂]²⁻ (Cᵢ)ᵈ		
	ν, cm⁻¹	scaledᵃ	I, km/mol	ν, cm⁻¹	scaledᵃ	I, km/mol	ν, cm⁻¹	scaledᵃ	I, km/mol
aₐ	3740	3067ᵇ	8	3744	3070ᵇ	0	3731	3059ᵇ	0
	2718	2229ᵇ	5	2649	2172ᵇ	0	2647	2171ᵇ	0.6
	2709	2221ᵇ	23	2587	2121ᵇ	31	2582	2117ᵇ	132
	1946	1596ᵇ	0	1896	1555ᵇ	0	1888	1548ᵇ	0
	1853	1519ᵇ	0	1772	1453ᵇ	0	1774	1455ᵇ	0
	1608	1447	0	1541	1387	0	1527	1374	0
	1505	1354	0	1517	1365	0	1509	1358	0
	1307	1176	0	1314	1183	0	1322	1190	0
	1118	1006	0	1202	1082	0	1200	1080	0
	904	814	0	907	816	0	1065	958	0
	728	655	0	778	700	0	909	818	0
	708	637	0	754	679	8	845	760	0
	635	572	0	659	593	0	773	696	0
	505	454	0	532	479	0	747	672	0
	359	323	0	366	329	0	664	598	0
	206	185	0	204	184	0	630	567	0
	180	162	3	185	166	0	561	505	0
	173	156	0	171	154	0	534	481	0
	116	104	0	116	104	0	441	397	0
bₐ	1081	973	0	1058	952	0	370	333	0
	878	790	0	830	747	0	259	233	0
	732	659	0	637	573	0	213	192	0
	513	462	0	557	501	0	184	166	0
	391	352	0	442	398	0	159	143	0
	256	230	0	256	230	0	137	123	0
	147	132	0	150	135	0	109	98	0
	38	34	0	23i	21i	0	29	26	0
aᵤ	1102	992	19	1069	962	21	3725	3054ᵇ	11
	804	724	3	714	643	30	2641	2166ᵇ	412
	667	600	1	628	565	105	2583	2118ᵇ	298
	535	482	2	557	501	0	1746	1484ᶜ	610
	459	413	2	505	454	1	1578	1420	346
	250	225	14	242	218	0	1461	1315	366
	98	88	8	96	86	6	1315	1184	85
	53	48	0	31	28	11	1288	1046	81
	15i	14i		22i	20i		1136	1022	266
bᵤ	3739	3066ᵇ	111	3736	3064ᵇ	12	1122	1010	310
	2719	2230ᵇ	37	2641	2166ᵇ	484	1072	965	23
	2710	2222ᵇ	39	2587	2121ᵇ	358	746	671	10
	1912	1568ᵇ	54	1750	1488ᶜ	719	725	652	12
	1902	1560ᵇ	74	1577	1419	473	641	577	101
	1609	1448	7	1466	1319	545	622	560	44
	1468	1321	10	1312	1181	25	599	539	17
	1279	1151	0	1291	1162	116	555	500	30
	1196	1076	73	1136	1022	524	511	460	5.9
	1121	1009	44	1125	1012	186	466	419	2.5
	713	642	1	754	679	8	264	238	1.4
	650	585	7	627	564	55	235	212	0.5
	598	538	6	615	553	15	181	163	18
	462	416	1	467	420	3	145	130	8.6
	251	226	2	246	221	0	95	86	7.2
	180	162	8	186	167	21	91	82	4.6
	155	140	2	154	139	4	32	29	11
	101	91	3	99	89	6	24	22	0.8

ᵃAll scale factors = 0.9 except for those labeled with b or c. ᵇScale factor = 0.82. ᶜScale factor = 0.85. ᵈSymmetry types for [TCNQI₂]²⁻ are aₐ and aᵤ.

Magnetic Susceptibility. The magnetic susceptibility, χ (defined as M/H), of [Fe(C₅Me₅)₂]⁺·[TCNQR₂]⁻ (R = Cl, Br, I, Me, OMe, OPh) and [Fe(C₅Me₅)₂]⁺·[TCNQMeCl]⁻ was measured between 2.2 and 300 K by the Faraday method.[10b] The data, Figure 8a, can be fit to a Curie–Weiss expression, $\chi_M = C/(T - \theta)$ with θ ranging from −6.2 to +9.5 K, Table I; the positive values are indicative of ferromagnetic coupling. The effective moment, μ_{eff}, calculated as $\mu_{eff} = [8\chi_M T]^{1/2}$ is shown as a function of temperature, Figure 8b, for this series of complexes. The effective moments range from 2.28–3.96 μ_B. This is consistent with a single spin per both the Fe site and a diamagnetic anion for the lower moment salts and is consistent with a spin per Fe and anion sites for the higher moment complexes, Table I. The quantitative assignment depends upon averaging the orientation dependent magnetic moment. The low value for the effective

moment for the [TCNQMe₂]⁻ and [TCNQ(OMe)₂]⁻ salts suggests the presence of singlet [TCNQR₂]₂²⁻ dimers as reported for the thermodynamically favored phase of [Fe(C₅Me₅)₂]⁺·[TCNQ]⁻²³ or more likely higher oligomers. The infrared spectra exhibit a broad base line dispersion indicative of a delocalized electron energy band characteristic of conducting or semiconducting materials. Thus, unpaired electrons on the anions may be in an electron energy band and contributes insignificantly to the susceptibility. The 3.64 μ_B moment for [Fe(C₅Me₅)₂]⁺·[TCNQ(OPh)₂]⁻ is consistent with unpaired electrons on both the cation and anion; however, the negative θ of −1.5 K is characteristic of weak antiferromagnetic not ferromagnetic coupling and was not studied further. Since, the [TCNQI₂]⁻ salt has the highest moment, the most positive value for θ as well as being the only member of this series of compounds with crystals suitable

Decamethylferrocene Electron-Transfer Salts

J. Am. Chem. Soc., Vol. 112, No. 14, 1990 5505

Figure 8. Inverse molar susceptibility, χ_M^{-1}, vs T(a, top) and effective moment, μ_{eff}, vs temperature, T, for $[Fe(C_5Me_5)_2]^{\cdot+}[TCNQR_2]^{\cdot-}$ [R = Cl (△), Br (O), I (□), Me (X), OMe (+), and OPh(*)] (b, bottom). Data were acquired at 19.6 kG.

for a complete single-crystal X-ray analysis we have studied its physical properties in detail. The crystals are, however, too small to determine the magnetic anisotropy.

The salt 2:1 salt $\{[Co(C_5Me_5)_2]^{\cdot+}\}_2[TCNQI_2]^{2-}$ was determined to be diamagnetic. The observed diamagnetic susceptibility was -590×10^{-6} emu/mol which is in agreement with expectation of -590×10^{-6} emu/mol calculated from the Pascal constants.

$[Fe(C_5Me_5)_2]^{\cdot+}[TCNQI_2]^{\cdot-}$ above 60 K obeys the Curie–Weiss law, $\chi_M = C/(T - \theta)$, Figure 8a. The parameters from a least-squares computer fit of χ_M^{-1} vs T give $\theta = +9.5$ K and $\mu_{eff} = 3.96$ μ_B. This value of μ_{eff} is consistent with two spins per metal atom, i.e., $S = 1/2$ $[Fe(C_5Me_5)_2]^{\cdot+}$ [with alignment of the powder sample with the chain axis parallel to the applied magnetic field $(g_\parallel \sim 4; g_\perp \sim 1.3)^{30}]$ and $S = 1/2$ $[TCNQI_2]^{\cdot-}$. The positive value of θ suggests a dominant ferromagnetic interaction. The plot of μ_{eff} vs T shows an increase in the data below 20 K and a maximum at 15 K prior to a drop in $\chi_M T$, Figure 8b.

The deviation from the Curie–Weiss law below 60 K shows that ferromagnetic interactions become less dominant at lower temperature. $[Fe(C_5Me_5)_2]^{\cdot+}[TCNQI_2]^{\cdot-}$ does not form a ferromagnetic ground state above 2.5 K. The magnetization, M, as a function of the applied field, H, at a temperature of 4.2 K is shown in Figure 9. Hysteresis was not observed at either 2.5 or 4.2 K. The field dependent magnetization at 4.2 K increases more rapidly than the simple classical Brillouin function for two unoriented $S = 1/2$ spins with a $g = 4^{30}$ for the $[Fe(C_5Me_5)_2]^{\cdot+}$ donor and $g = 2$ for the anion, Figure 8. The $M(H)$ is fit by the Brillouin
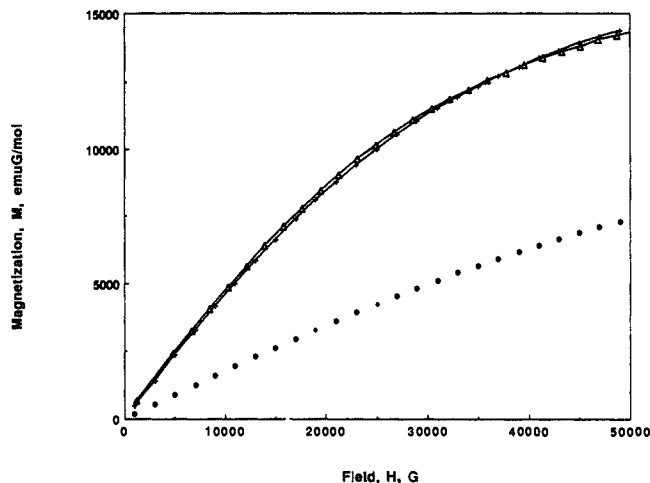
Figure 9. Field dependence magnetization, M(H), for $[Fe(C_5Me_5)_2]^{\cdot+}[TCNQI_2]^{\cdot-}$ at 4.2 K. Calculated for $g = 2$ and $g = 4.15$ spins (+), 2 g = 2 spins (●), and observed data (△).

function if complete alignment of the spins with ($g = 4$ parallel to H) the magnetic field is assumed. This suggests that either microcrystals are aligned parallel to the magnetic field with no cooperative effects at 4.2 K or the samples exhibit an enhanced magnetization which coincidentally fits the data expected for fully aligned samples. If the latter is correct, then below 2.5 K a large ferromagnetic coupling should be observed. This is consistent with magnetic ordering suggested by the zero field Mössbauer spectrum at 1.5 K. The $M(H)$ and $\chi(T)$ behaviors are in agreement with 1-D ferromagnetic interactions above 60 K along the ··· $D^{\cdot+}A^{\cdot-}D^{\cdot+}A^{\cdot-}$··· chains as observed for $[Fe(C_5Me_5)_2]^{\cdot+}[TCNE]^{\cdot-}$ and $[Fe(C_5Me_5)_2]^{\cdot+}[TCNQ]^{\cdot-}$ and a weaker 3-D interchain interaction between the chains. The presence of a ferromagnetic ground state depends on the existence of inter- as well as intrachain ferromagnetic exchange. The formation of a 3-D ferromagnetic ground state in these electron-transfer compounds could be hindered by the interchain coupling being net antiferromagnetic as is expected with increased interchain acceptor–acceptor interactions. The $[TCNQI_2]^{\cdot-}$ is larger than $[TCNQ]^{\cdot-}$ which in turn is larger than $[TCNE]^{\cdot-}$, and it orients differently than the anions in the $[Fe(C_5Me_5)_2]^{\cdot+}[TCNE]^{\cdot-}$ and $[Fe(C_5Me_5)_2]^{\cdot+}[TCNQ]^{\cdot-}$ salts so that the net interchain exchange (sum of the $D^{\cdot+}/D^{\cdot+}$ and $D^{\cdot+}/A^{\cdot-}$ ferromagnetic and $A^{\cdot-}/A^{\cdot-}$ antiferromagnetic) interaction is now antiferromagnetic. This would suppress 3-D ferromagnetic ordering. Comparison of the Curie–Weiss θ (which primarily reflects the 1-D exchange) between that of $[Fe(C_5Me_5)_2]^{\cdot+}[TCNE]^{\cdot-}$ ($\theta = +30$ K)[9a] and that of $[Fe(C_5Me_5)_2]^{\cdot+}[TCNQI_2]^{\cdot-}$ ($\theta = +9.5$ K) suggests a weaker intrachain exchange interaction in the latter salt arising from a poorer intrachain transfer integral between $[Fe(C_5Me_5)_2]^{\cdot+}$ and $[TCNQI_2]^{\cdot-}$ as compared with that of the $[TCNE]^{\cdot-}$ salt. The small θ (+3 K) for the metamagnetic $[TCNQ]^{\cdot-}$ salt is even lower[5] reflecting even weaker exchange along the chain. The metamagnetic behavior in the $[TCNQ]^{\cdot-}$ salt below 2.55 K may reflect that the net interchain exchange (sum of the $D^{\cdot+}/D^{\cdot+}$ and $D^{\cdot+}/A^{\cdot-}$ ferromagnetic and $A^{\cdot-}/A^{\cdot-}$ antiferromagnetic interactions) is slightly antiferromagnetic and that the salt switches to the ferromagnetic state in a small magnetic field.

Conclusion

The best available conceptual framework to view the stabilization of ferromagnetic coupling in molecular based donor/acceptor complexes is based upon the extended[7b,31] McConnell mechanism.[32] Besides the obvious necessity of having unpaired spins at various sites, the long-range order of these spins is important. Within this McConnell model, the stabilization of ferromagnetic coupling arises from the configurational mixing of a

(30) Duggan, D. M.; Hendrickson, D. N. *Inorg. Chem.* **1975**, *14*, 955. Morrison, W. H., Jr.; Krogsrud, S.; Hendrickson, D. N. *Inorg. Chem.* **1973**, *12*, 1998. Morrison, W. H., Jr.; Hendrickson, D. N. *Inorg. Chem.* **1975**, *14*, 2331.

(31) Miller, J. S.; Epstein, A. J. *J. Am. Chem. Soc.* **1987**, *109*, 3850.
(32) McConnell, H. M. *Proc. Robert A. Welch Found. Chem. Res.* **1967**, *11*, 144.

5506 *J. Am. Chem. Soc., Vol. 112, No. 14, 1990*

Miller et al.

charge transfer excited state with the ground state. The model predicts that for excitation from the HOMO of a donor with three electrons in a doubly degenerate HOMO, d^3 {e.g., for [Fe-$(C_5Me_5)_2$]$^{*+}$}, to an acceptor with a half-filled nondegenerate HOMO, s^1 {e.g., from [TCNE]$^{*-}$}, ferromagnetic coupling is stabilized. Likewise, disproportionation via excitation among the d^3 donors stabilizes ferromagnetic coupling. In contrast, disproportionation via excitation from the s^1 acceptor stabilizes antiferromagnetic coupling. Thus, the observed magnetic behavior is a consequence of the competing ferromagnetic (s^1/d^3, d^3/d^3) and antiferromagnetic (s^1/s^1) interactions.

In order to obtain a qualitative understanding of the relative importance of the antiferromagnetic s^1/s^1 as well as the ferromagnetic s^1/d^3 and d^3/d^3 interactions, the interion distances between the atoms with the greatest spin density (Fe and N) are compared. For the ferromagnetic d^3/d^3 intrachain interactions, the Fe⋯Fe distances are slightly longer in the [TCNQI$_2$]$^{*-}$ salt (11.13 Å) as compared to the metamagnetic [TCNQ]$^{*-}$ salt (10.55 Å); however, ferromagnetic intrachain interactions have also been noted for similarly structured [Fe($C_5Me_5)_2$]$^{*+}$ salts with Fe⋯Fe distances as long as 12.10 Å.[11] The interchain Fe⋯Fe distances are comparable for the [TCNQI$_2$]$^{*-}$ and the [TCNQ]$^{*-}$ salts with the distances for the [TCNQ]$^{*-}$ salt again being slightly shorter. The interchain Fe⋯N (s^1/d^3 interaction) distances are significantly shorter than the intrachain distances suggesting that the former should be a more important effect. The interchain Fe⋯N distances are comparable for [TCNQI$_2$]$^{*-}$ and [TCNQ]$^{*-}$ salts with those for the [TCNQI$_2$]$^{*-}$ salt being shorter. The shortest distance in the [TCNQI$_2$]$^{*-}$ salt is 5.11 Å as compared to 5.25 Å in the [TCNQ]$^{*-}$ salt. The intrachain Fe⋯N distances in the [TCNQ]$^{*-}$ salt are significantly shorter than in the [TCNQI$_2$]$^{*-}$ salt with the shortest distance being 6.10 Å in the former as compared to 6.96 Å in the latter. This is in part a consequence of the longer Fe⋯Fe intrachain distance in the latter although tilting of the anion also contributes.

The most significant difference in the distances occurs for the antiferromagnetic s^1/s^1 interchain anion–anion N⋯N interactions. The N⋯N interchain distances are significantly longer in the [TCNQI$_2$]$^{*-}$ salt (5.24 Å) as compared to the [TCNQ]$^{*-}$ salt (3.92 Å). Since this is an antiferromagnetic interaction, this suggests that the [TCNQI$_2$]$^{*-}$ salt would have greater net interchain ferromagnetic interactions. However, the I⋯N in the [TCNQI$_2$]$^{*-}$ salt and H⋯N distances in the [TCNQ]$^{*-}$ salt are significantly shorter. The shortest N⋯H distance in the [TCNQ]$^{*-}$ salt is 2.53 Å which is expected for a weak CH⋯N hydrogen bond with the other distance being much longer (3.43 Å) and greater than the

sum of the van der Waals radii.[26] In the [TCNQI$_2$]$^{*-}$ salt, there are two very short N⋯I interactions of 3.12 and 3.15 Å for the in-registry anions (Figures 3a and 4) and much longer ones of at least of 5.2 Å for the out-of-registry anions (Figure 3b and c). The short N⋯I bond is significantly less than the sum of the van der Waals radii which ranges from 3.5 to 3.7 Å.[26] Clearly this is a very strong I⋯N interaction presumably due to the high polarizability of the iodine atom.[33] In the [TCNQI$_2$]$^{*-}$ salt the two [TCNQI$_2$]$^{*-}$ radicals are slipped, Figure 4, enabling two strong N⋯I interactions as compared to the [TCNQ]$^{*-}$ salt which does not require as large a slippage in order to have two good H⋯N interactions. Although I, like H, does not have excess spin or charge, it is very polarizable and could have large interactions with the large excess spin and charge on the N of the cyano group. These strong N⋯I interactions could lead to increased antiferromagnetic coupling between the chains thereby decreasing the ability of the material to have proper net coupling between the chains and destroying bulk ferromagnetism. In contrast the H in TCNQ is a much weaker polarizing species and will have a much weaker interaction with the excess spin and charge on the cyano N. Thus it is likely that the interchain anion–anion interactions lead to the differences in the bulk magnetic behavior of the [TCNQI$_2$]$^{*-}$ and [TCNQ]$^{*-}$ salts.

(33) Desiragu, D.; Harlow, R. L. *J. Am. Chem. Soc.* **1989**, *111*, 6754.
(34) Chem-X was modified for use at Du Pont and was developed and distributed by Chemical Design Ltd., Oxford, UK.